

# Analysis and Design of a High-Stability, High-Accuracy, Low-Dropout Voltage Regulator

Shen Liangguo<sup>1,†</sup>, Yan Zushu<sup>2</sup>, Wang Zhao<sup>3</sup>, Zhang Xing<sup>1</sup>, and Zhao Yuanfu<sup>2</sup>

(1 Institute of Microelectronics, Peking University, Beijing 100871, China)

(2 Beijing Microelectronics Technology Institute, Beijing 100076, China)

(3 Vimicro Corporation, Beijing 100083, China)

**Abstract:** A high-accuracy, low-dropout (LDO) voltage regulator is presented. Using the slow-rolloff frequency compensation scheme, the LDO effectively overcomes the stability problem, facilitates the use of a ceramic capacitor, and improves the output voltage accuracy, which is critical for powering high-performance analog circuitry. The slow-rolloff compensation scheme is realized by introducing three pole-zero pairs, including the proposed pole-zero pair and sense zero. The post-layout simulation results demonstrate that this LDO has robust system stability, a high open-loop gain, and a high unit-gain frequency, which lead to excellent regulation and transient response performance. The line and load regulation are  $27\mu\text{V}/\text{V}$  and  $3.78\mu\text{V}/\text{mA}$ , and the overshoots of the output voltage are less than  $30\text{mV}$ , while the dropout voltage is  $120\text{mV}$  for a  $150\text{mA}$  load current.

**Key words:** voltage regulator; LDO; slow-rolloff frequency compensation; line regulation; load regulation

**EEACC:** 1205; 1210

**CLC number:** TN432

**Document code:** A

**Article ID:** 0253-4177(2007)12-1872-06

## 1 Introduction

The low-dropout (LDO) voltage regulator is a vital part of an electronic system. One of the issues in LDO design is to maintain system stability<sup>[1]</sup>. Besides degrading the load transient response performance, the conventional equivalent series resistance (ESR) frequency compensation technique relies heavily on the ESR value of the output capacitor, which is not properly specified and varies with temperature<sup>[2]</sup>. The commonly used Miller compensation scheme, however, is not efficient for LDOs because of the large variance of the load impedance and the output capacitor of the LDO<sup>[3]</sup>.

Another issue is to improve the line/load regulation and transient response performance, which requires high DC open-loop gain and unit-gain frequency (UGF). Although the internal zeros were introduced in Refs. [4, 5], they are still not sufficient for the requirements mentioned above. Furthermore, in order to generate these zeros, an extra quiescent current is required.

To circumvent these difficulties, the LDO

presented in this paper employs the slow-rolloff compensation scheme<sup>[6,7]</sup>. This scheme not only enhances the stability effectively, but also aids in the design of a high-gain, high-accuracy LDO. The slow-rolloff compensation topology is realized by three pole-zero pairs, including a proposed sense zero and a novel pole-zero pair. The sense zero can replace the conventional ESR zero and make the use of a low ESR ceramic output capacitor possible. Since it is embedded in the differential input stage of the error amplifier, the pole-zero pair generation circuit does not consume any additional power.

## 2 Pole-zero pair and sense zero generation circuit

The proposed pole-zero pair generation circuit is shown in Fig. 1(a). In this figure,  $V_o$  is the output voltage of the differential input stage,  $V_i/2$  and  $-V_i/2$  are the differential input signals, while  $R$  and  $C$  function as pole-zero pair generation components.

Figure 1(b) presents the small-signal model of this circuit, where  $C_{gd3}$  and  $C_{gd4}$  are the gate-

† Corresponding author. Email: shenliangguo@gmail.com

Received 12 June 2007, revised manuscript received 1 August 2007

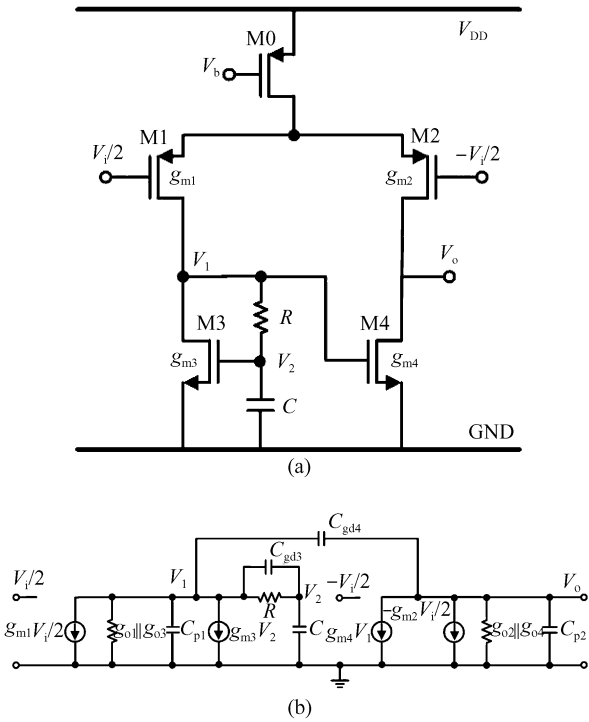


Fig. 1 (a) Pole-zero pair generation circuit; (b) Small-signal model

drain parasitic capacitances of M3 and M4, while  $g_{m1} \sim g_{m4}$  and  $g_{o1} \sim g_{o4}$  are the transconductances and output conductances of transistors M1~M4.  $C_{p1}$  and  $C_{p2}$  are the parasitic capacitances from node  $V_1$  and  $V_o$  to ground, respectively.

The transfer function is given by Eq. (1). Here, the following approximations have been made:  $g_{m1} = g_{m2}$ ,  $g_{m3} = g_{m4}$ ;  $g_{m3}R > 1$ ;  $C \gg C_{p1}, C_{p2}$ ,  $g_{m3}RC_{gd3}$ ;  $C_{p1}, C_{p2} \gg C_{gd3}, C_{gd4}$ .

$$\frac{v_o(s)}{v_i(s)} \approx \frac{g_{m1}}{g_{o2} + g_{o4}} \times \frac{\left(1 + s \frac{(1 + g_{m3}R)C}{2g_{m3}}\right) \left(1 + s \frac{RC_{p1}}{1 + g_{m3}R}\right)}{1 + s \left(\frac{C_{p2}}{g_{o2} + g_{o4}} + \frac{C}{g_{m3}}\right) + s^2 \frac{C_{p2}C}{(g_{o2} + g_{o4})g_{m3}} + s^3 \frac{C_{p2}CRC_{p1}}{(g_{o2} + g_{o4})g_{m3}}} \quad (1)$$

The zeros in Eq. (1) are given below:

$$\omega_{z1} = \frac{2g_{m3}}{(1 + g_{m3}R)C} \quad (2)$$

$$\omega_{z2} = \frac{1 + g_{m3}R}{RC_{p1}} \quad (3)$$

Under the conditions of  $C_{p2}/(g_{o2} + g_{o4}) \gg C/g_{m3}$  and  $C \gg g_{m3}RC_{p1}$ , the poles in Eq. (1) become:

$$\omega_{p1} = \frac{g_{o2} + g_{o4}}{C_{p2}} \quad (4)$$

$$\omega_{p2} = \frac{g_{m3}}{C} \quad (5)$$

$$\omega_{p3} = \frac{1}{RC_{p1}} \quad (6)$$

The required pole-zero pair is composed of

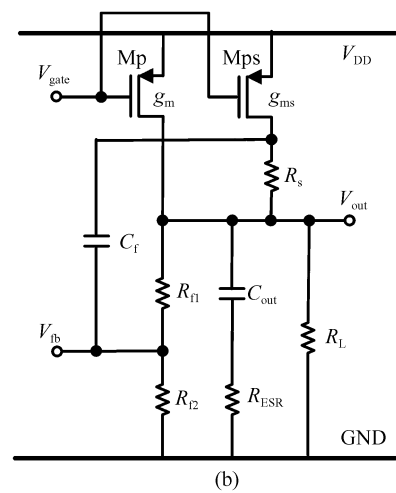
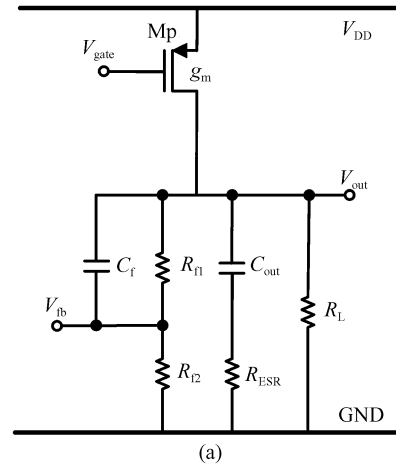


Fig.2 (a) ESR zero generation circuit; (b) Sense zero generation circuit

the zero  $\omega_{z1}$  and pole  $\omega_{p2}$ . When  $g_{m3}R = 7$ , the frequency of the zero  $\omega_{z1}$  is 4 times lower than that of the pole  $\omega_{p2}$ . Thus, the phase shift of the feedback loop can be effectively reduced at specific frequency ranges.

This pole-zero pair generation circuit has three advantages: First, the circuit realization is simple and only needs two passive components; Second, although embedded in the differential input stage, these components do not change the DC operation state of the input stage; Third, no extra quiescent current is needed, which is critical for portable electronic applications.

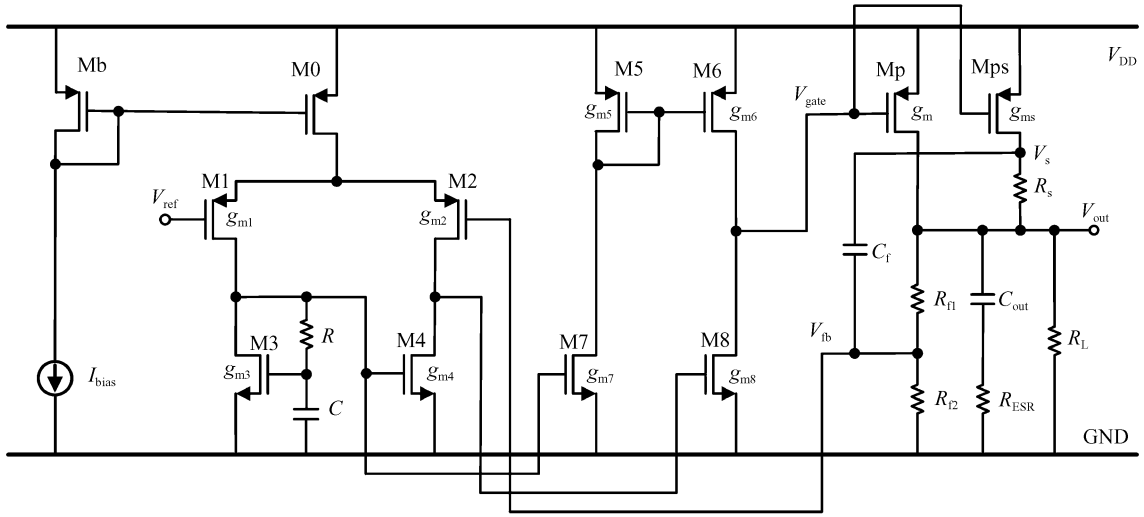


Fig.3 Circuit implementation of the LDO core

Figure 2 gives the ESR zero and sense zero generation circuits. The former is the conventional structure, while the latter is the topology proposed in this paper. Mp is the power transistor, Mps is the sense transistor, while  $g_m$  and  $g_{ms}$  are the transconductances of Mp, Mps.  $V_{gate}$ ,  $V_{out}$ ,  $V_{fb}$  are the power transistor gate control voltage, the output voltage and the feedback voltage, respectively. The output capacitor  $C_{out}$  and associated ESR, and the lumped load resistance  $R_L$  are also included.

In Fig. 2(a), the transfer function from  $V_{gate}$  to  $V_{fb}$  is characterized by two zeros and two poles:

$$\omega_{Z3} = \frac{1}{R_{f1} C_f} \quad (7)$$

$$\omega_{Z4} = \frac{1}{R_{ESR} C_{out}} \quad (8)$$

$$\omega_{P4} = \frac{R_{f1} + R_{f2} + R_L}{(R_{f1} + R_{f2}) R_L C_{out}} \quad (9)$$

$$\omega_{P5} = \frac{R_{f1} + R_{f2}}{R_{f1} R_{f2} C_f} \quad (10)$$

In Fig. 2 (b), the resistor  $R_s$  senses the drain current of Mps, while the feedback capacitor  $C_f$  not only forms another pole-zero pair with the feedback resistors  $R_{f1}$ ,  $R_{f2}$ , but also senses the drain voltage of Mps and helps to generate a sense zero. In the corresponding transfer function of Fig. 2 (b), with the assumptions of  $g_m \gg g_{ms}$ ;  $R_{f1} \gg R_s$ ;  $(R_{f1} + R_{f2})^2 R_L C_{out} \gg R_{f1} R_{f2} (R_{f1} + R_{f2} + R_L) \times C_f$  and  $R_{f1} C_f \gg (R_s g_{ms}/g_m + R_{ESR}) C_{out}$ , the sense zero  $\omega_{Z4}$  can be approximated to:

$$\omega_{Z4} \approx \frac{1}{(R_s g_{ms}/g_m + R_{ESR}) C_{out}} \quad (11)$$

If  $R_s g_{ms}/g_m \gg R_{ESR}$ , then  $\omega_{Z4}$  reduces to:

$$\omega_{Z4} \approx \frac{1}{(R_s g_{ms}/g_m) C_{out}} \quad (12)$$

The other zero and poles are the same as that shown in Eqs. (7,9,10).

The aspect ratio of Mp is 1000 times larger than that of Mps. The current cross  $R_s$  (300Ω in this design) is 150μA under a full load (the current across Mp is about 150mA), thus the voltage drop on  $R_s$  is small (45mV). Therefore, the Mps has almost the same operational state as Mp, which means that  $g_m \approx 1000 g_{ms}$ .

Under this condition, the sense zero with  $R_s g_{ms}/g_m$  equals 300mΩ and has the same function as the ESR zero with the ESR value of 300mΩ. In other words, the sense zero can replace the ESR zero, which facilitates the use of low-ESR (typically less than 50mΩ), low-cost, and compact ceramic capacitors and improves the load transient responses.

The current in Mps flows to the load, thus the sense-zero generation circuit does not increase the power of the LDO.

### 3 Circuit and layout realization of the LDO

The circuit diagram of the LDO core is shown in Fig. 3. It contains the first gain stage (consisting of M0 ~ M4,  $R$ ,  $C$ ), the second gain stage (consisting of M5 ~ M8), and the sense zero generation circuit (which also is the third gain

stage of the LDO). Based on the topology presented in Ref. [8], the bandgap circuit provides the reference voltage and bias current for the LDO core. The reference voltage ( $V_{ref}$ ) of 0.3V is adopted because it is suitable for low supply voltage applications and required by the slow-rolloff compensation scheme.

### 3.1 Stability and accuracy improvement

Besides the zeros  $\omega_{z1} \sim \omega_{z4}$  and poles  $\omega_{p1} \sim \omega_{p5}$  mentioned above, other poles of the LDO are given by

$$\omega_{p6} = \frac{1}{R_{gate} C_{gate}} \quad (13)$$

$$\omega_{p7} = \frac{1}{R_{f2} C_{fb}} \quad (14)$$

Here,  $R_{gate}$ ,  $C_{gate}$  are the output resistance and the lumped parasitic capacitance of the node  $V_{gate}$ , while  $C_{fb}$  is the lumped parasitic capacitance of the node  $V_{fb}$  to ground, which is mainly composed of the gate-source capacitance of the transistor M2.

Dominant-pole compensation scheme involves a dominant pole (the output pole  $\omega_{p4}$ ), so any additional poles potentially degrade the phase margin<sup>[4,5]</sup>. This scheme has three drawbacks. First, the pole  $\omega_{p6}$  is usually located in the UGF, thus a compensation zero is necessary. However, an accurate pole-zero cancellation is difficult to achieve because  $\omega_{p6}$  is highly variable relied on the operational region of the power transistor Mp, which is determined by the load conditions and the supply voltage. Second, the internal pole  $\omega_{p1}$  should be at a significantly higher frequency than the UGF, which restricts the achievable UGF and loop gain. Third, high dc gain and high UGF cannot be achieved simultaneously because of the single-pole roll-off characteristic.

In such cases, slow-rolloff compensation offers a valuable option. A dominant half-pole, whose magnitude rolls off as the square root of frequency and whose phase lag is  $45^\circ$ <sup>[7]</sup>, is approximately implemented by the pole  $\omega_{p6}$  and three pole-zero pairs. The first pole-zero pair is achieved by zero  $\omega_{z3}$  and pole  $\omega_{p5}$ , the second is  $\omega_{z4}$  and  $\omega_{p1}$ , while the third is  $\omega_{z1}$  and  $\omega_{p2}$ . In addition,  $\omega_{z3}$ ,  $\omega_{p5}$ ,  $\omega_{z4}$ ,  $\omega_{p1}$ ,  $\omega_{z1}$  and  $\omega_{p2}$  distribute alternately with an almost constant frequency ratio 4. The phase lag of this dominant half-pole is  $45^\circ$ , while the in-band output pole  $\omega_{p4}$  contributes at

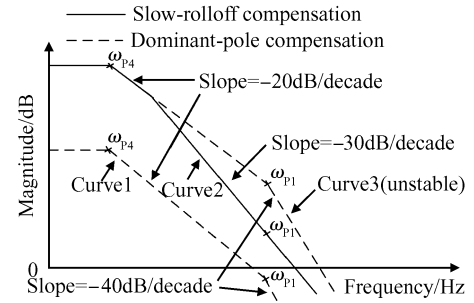


Fig.4 Comparison of slow-rolloff and dominant-pole compensation

most a  $90^\circ$  phase lag, so that the worst-case phase margin of the proposed LDO is  $45^\circ$ .

The UGF of the slow-rolloff compensation LDO can be well above the internal pole  $\omega_{p1}$ , because this pole is included in the pole-zero pairs. The primary advantage of the proposed LDO is that high loop gain and high UGF can be obtained at the same time. As shown in Fig. 4, compared to the dominant-pole compensation (curve 1), the slow-rolloff compensation (curve 2) achieves a much higher loop gain (especially at DC and low-frequency, which is critical for improving regulation performance) and a higher UGF (which translates to fast transient response). Curve 3 has the same DC gain as curve 2, but at the cost of potential instability.

The high-frequency poles  $\omega_{p3}$ ,  $\omega_{p7}$  and zero  $\omega_{z2}$  can be ignored because they are well above the UGF of the LDO.

### 3.2 Layout implementation of the whole LDO

Figure 5 shows the layout of the whole LDO, which includes the LDO core, the power transistor, the bandgap reference, the current limiter, and the overheat protector.

During layout design, the device matching and the impact of device parasitic capacitance on circuit performance were taken into consideration. For instance, the capacitor  $C_f$  used in the LDO core is realized by a poly1-poly2 capacitor, whose lower electrode is connected to node  $V_s$ , which is not sensitive to the parasitic capacitance.

## 4 Post-layout simulation results of the LDO

The LDO was simulated using HSPICE and a

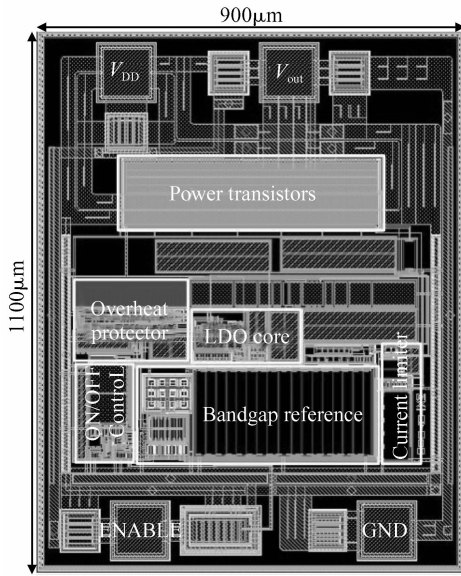


Fig. 5 Layout of the LDO

commercial  $0.5\mu\text{m}$  CMOS double poly mixed-signal process model from CSMC Technologies Corporation. The supply voltage ( $V_{in}$ ) varies from 1.8 to 5.5V, and the output voltage is 1.5V.  $C_{out} = 1\mu\text{F}$ ,  $R_s = 300\Omega$ ,  $R_{f1} = 480\text{k}\Omega$ ,  $R_{f2} = 120\text{k}\Omega$ ,  $C_f = 10\text{pF}$ ,  $R = 180\text{k}\Omega$ ,  $C = 1\text{pF}$ .

4.1 Frequency responses and phase margin

Figure 6 presents the frequency response characteristics of the LDO at  $V_{in} = 1.8\text{V}$  and  $V_{in} = 5.5\text{V}$ , respectively, while  $R_{ESR} = 0$ . The UGF is located in the range of  $306\text{kHz} \sim 3.13\text{MHz}$  when  $I_{out}$  varies from 1 to 150mA, while the phase margin is better than  $45^\circ$  for all cases.

Figure 7 gives the phase margin versus load current curves of the proposed LDO at supply voltages of 1.8V and 5.5V. An  $R_{ESR}$  range of 0 to  $0.3\Omega$  was used in the simulation, which is sufficient to account for the  $R_{ESR}$  variance of the multilayer ceramic capacitor.

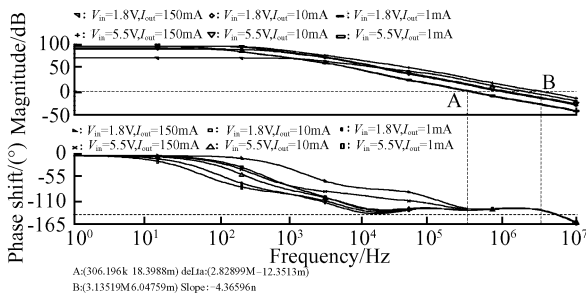


Fig.6 Frequency response curves of the LDO at  $V_{in} = 1.8\text{V}$  and  $5.5\text{V}$

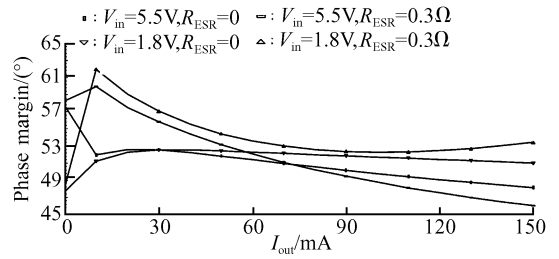


Fig. 7 Phase margin versus load current of the LDO

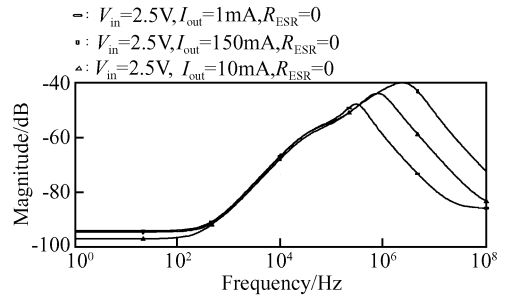


Fig. 8 PSR characteristics of the LDO at  $V_{in} = 2.5\text{V}$ ,  $V_{out} = 1.5\text{V}$

The phase margin is higher than  $45^\circ$  at the four extreme cases, which demonstrates that this compensation scheme is valid over the entire load current range and suitable for the use of a ceramic output capacitor.

4.2 Power supply rejection (PSR) characteristics

The PSR characteristics of the LDO are given in Fig. 8. The supply voltage is 2.5V, which corresponds to the PSR test condition of  $V_{in} = V_{out} + 1\text{V}$ . The PSR values are higher than 93, 85, 66, 55, and 42dB at DC, 1kHz, 10kHz, 100kHz and 1MHz, respectively.

4.3 Load transient response

Figure 9 shows that, when the load current changes between 0 and 150mA in  $5\mu\text{s}$ , the overshoot and undershoot of the output voltage both are less than 30mV.

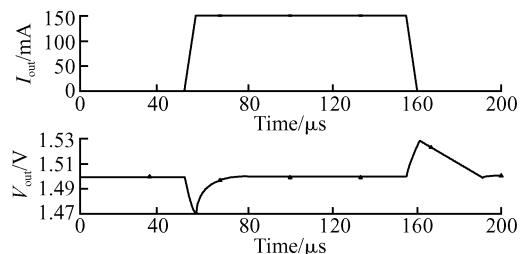


Fig.9 Load transient response of the LDO at  $V_{in} = 1.8\text{V}$ ,  $V_{out} = 1.5\text{V}$

Table 1 Summary of the post-layout simulation results

Technology	CSMC 0.5 $\mu$ m CMOS
Threshold voltage	$V_{thn} \approx 0.75V$ , $V_{thp} \approx -1.02V$
Chip area	1100 $\mu$ m $\times$ 900 $\mu$ m
Supply voltage range	1.8~5.5V
Output voltage range	1.5~5.2V
Ground current	32.5 $\mu$ A
Output current range	0~150mA
Output capacitor	1 $\mu$ F or above ceramic capacitor
Dropout voltage	120mV@150mA, $V_{out} = 1.5V$
DC open-loop gain	70~100dB
Line regulation	27 $\mu$ V/V@ $I_{out} = 150mA$
Load regulation	3.78 $\mu$ V/mA@ $V_{in} = 1.8V$
Overshoot & Undershoot	< 30mV
PSR @ $V_{in} = 2.5V$	93dB@DC, 42dB@1MHz

Table 1 summarizes the performance of the LDO. A dropout voltage of 120mV is achieved at the 150mA maximum load current. Owing to the high open-loop DC gain guaranteed by the slow-rolloff compensation, the line and load regulation are only 27 $\mu$ V/V and 3.78 $\mu$ V/mA.

## 5 Conclusion

The design of a high-accuracy LDO based on a slow-rolloff frequency compensation scheme is presented in this article. Besides the detailed description of the proposed pole-zero pair and the sense zero, the stability analysis and the method of

accuracy improvement of the slow-rolloff compensation LDO have been given. The post-layout simulation results confirmed that this LDO is highly-stable under various supply voltages, ESR values, and load conditions. In addition, excellent line/load regulation and transient response performances can be achieved. This paper offers a novel approach for achieving pole-zero pairs without increasing the quiescent power.

## References

- [1] Rincon-Mora G A, Allen P E. A low-voltage, low quiescent current, low drop-out regulator. *IEEE J Solid-State Circuits*, 1998, 33:36
- [2] ESR, stability, and the LDO regulator. Texas Instruments, Dallas, TX, Texas Instruments Data Sheet, REG115, 2002
- [3] Lau S K, Mok P K T, Leung K N. A low-dropout regulator for SoC with Q-reduction. *IEEE J Solid-State Circuits*, 2007, 42(3):658
- [4] Chava C K, Silva-Martinez J. A frequency compensation scheme for LDO voltage regulators. *IEEE Trans Circuit Syst I*, 2004, 51:1041
- [5] Shen L G, Yan Z S, Zhang X, et al. Design of high-performance voltage regulators based on frequency-dependent feedback factor. *IEEE International Symposium on Circuits and Systems*, New Orleans, USA, 2007, 3828
- [6] Roberge J K. *Operational amplifiers: theory and practice*. New York: Wiley, 1975
- [7] Lee T H. *The design of CMOS radio-frequency integrated circuits*. 2nd ed. Cambridge University Press, 2004
- [8] Neuteboom H, Kup B M J, Jansses M. A DSP-based hearing instrument IC. *IEEE J Solid-State Circuits*, 1997, 32:1790

## 一种高稳定性高精度低压差线性稳压器的分析与设计

沈良国<sup>1,†</sup> 严祖树<sup>2</sup> 王 钊<sup>3</sup> 张 兴<sup>1</sup> 赵元富<sup>2</sup>

(1 北京大学微电子学系, 北京 100871)

(2 北京微电子技术研究所, 北京 100076)

(3 中星微电子有限公司, 北京 100083)

**摘要:** 提出了 LDO, 其基于缓慢滚降式频率补偿方法, 通过在电路中引入三个极零对(极零对的产生没有增加静态功耗), 不仅克服了常规 LDO 不能使用低等效串联电阻、低成本陶瓷输出电容的缺点, 而且确保了系统在整个负载和输入电压变化范围内稳定工作. 由于 LDO 通常给高性能模拟电路供电, 因此其输出电压精度至关重要; 而该补偿方法能满足高环路增益、高单位增益带宽的设计要求, 从而大幅提高 LDO 的精度. 该 LDO 基于 0.5 $\mu$ m CMOS 工艺实现. 后仿结果表明, 即使在低压满负载条件下, 其开环 DC 增益仍高于 70dB, 满载时单位增益带宽可达 3MHz, 线性调整率和负载调整率分别为 27 $\mu$ V/V 和 3.78 $\mu$ V/mA, 过冲和欠冲电压均小于 30mV, 负载电流为 150mA 时的漏失电压(dropout 电压)仅为 120mV.

**关键词:** 线性稳压器; 低压差; 缓慢滚降式频率补偿; 线性调整率; 负载调整率

EEACC: 1205; 1210

中图分类号: TN432

文献标识码: A

文章编号: 0253-4177(2007)12-1872-06

† 通信作者. Email: shenliangguo@gmail.com

2007-06-12 收到, 2007-08-01 定稿